The Geological Society of America
Special Paper 444
2008

Timing and distribution of tectonic rotations in the northeastern Tibetan Plateau

Guillaume Dupont-Nivet*
Paleomagnetic Laboratory "Fort Hoofddijk," Utrecht University, 3584 CD Utrecht, Netherlands

Shuang Dai
Key Laboratory of Western China's Environmental Systems, Ministry of Education of China & College of Resources and Environment, Lanzhou University, Gansu 730000, China

Xiaomin Fang
Institute of Tibetan Plateau Research, Chinese Academy of Science, P.O. Box 2871, Beijing 100085, China, and
Key Laboratory of Western China's Environmental Systems, Ministry of Education of China & College of Resources and Environment, Lanzhou University, Gansu 730000, China

Wout Krijgsman
Veronique Erens
Mariel Reitsma
Cor Langereis
Paleomagnetic Laboratory "Fort Hoofddijk," Utrecht University, 3584 CD Utrecht, Netherlands

ABSTRACT

We report paleomagnetic data from the northeastern margin of the Tibetan Plateau to help understand the timing and distribution of deformation (i.e., vertical-axis rotations) during the India-Asia collision. Paleomagnetic results throughout Xining Basin strata, recently dated using magnetostratigraphy to between 52 and 17 Ma, show that some 25° of clockwise rotation with respect to the stable Eurasian continent occurred at ca. 41 Ma. In view of a regional compilation of existing paleomagnetic data from the northeastern Tibetan Plateau, these results suggest that this region experienced clockwise rotations in the regional Paleocene-Miocene basin system, including rotation in the Xining Basin, ca. 41 Ma, thus establishing the existence of widespread deformation at this time. During a mid-Miocene phase, between 17 and 11 Ma, clockwise rotations were restricted to the Miocene-Quaternary basin system, implying that the Laji Shan thrust belt, which separates the two basin systems, was active during this time interval.

Keywords: tectonic rotations, paleomagnetism, Tibetan Plateau, Cenozoic.

*gdn@geo.uu.nl.

Dupont-Nivet, G., Dai, S., Fang, X., Krijgsman, W., Erens, V., Reitsma, M., and Langereis, C., 2008, Timing and distribution of tectonic rotations in the northeastern Tibetan Plateau, *in* Burchfiel, B.C., and Wang, E., eds., Investigations into the Tectonics of the Tibetan Plateau: Geological Society of America Special Paper 444, p. 73–87, doi: 10.1130/2008.2444(05).

INTRODUCTION

The world's largest and highest orogenic system results from the collision and northward indentation of India into Asia since the Eocene (Argand, 1924; Yin and Harrison, 2000) (Fig. 1). The timing and mechanism of tectonic deformation have important implications for understanding lithospheric behavior in a continental collision setting, and for the possible impacts of uplift on regional and global climate (Molnar et al., 1993; Tapponnier et al., 2001; Ruddiman et al., 1997). Using paleomagnetism and quantitative determinations of tectonic rotations about a vertical axis we can test geodynamic models describing the kinematics of the India-Asia collision system (Avouac and Tapponnier, 1993; Holt et al., 2000; Dupont-Nivet et al., 2002a, 2003). A growing paleomagnetic data set provides first-order information showing that significant rotations are concentrated mainly along the margins of the deforming region in the western and eastern syntaxis (Dupont-Nivet et al., 2003). Unfortunately, precise age determinations of this component of deformation remain hindered by poor age control on the rocks studied, such that it is still difficult

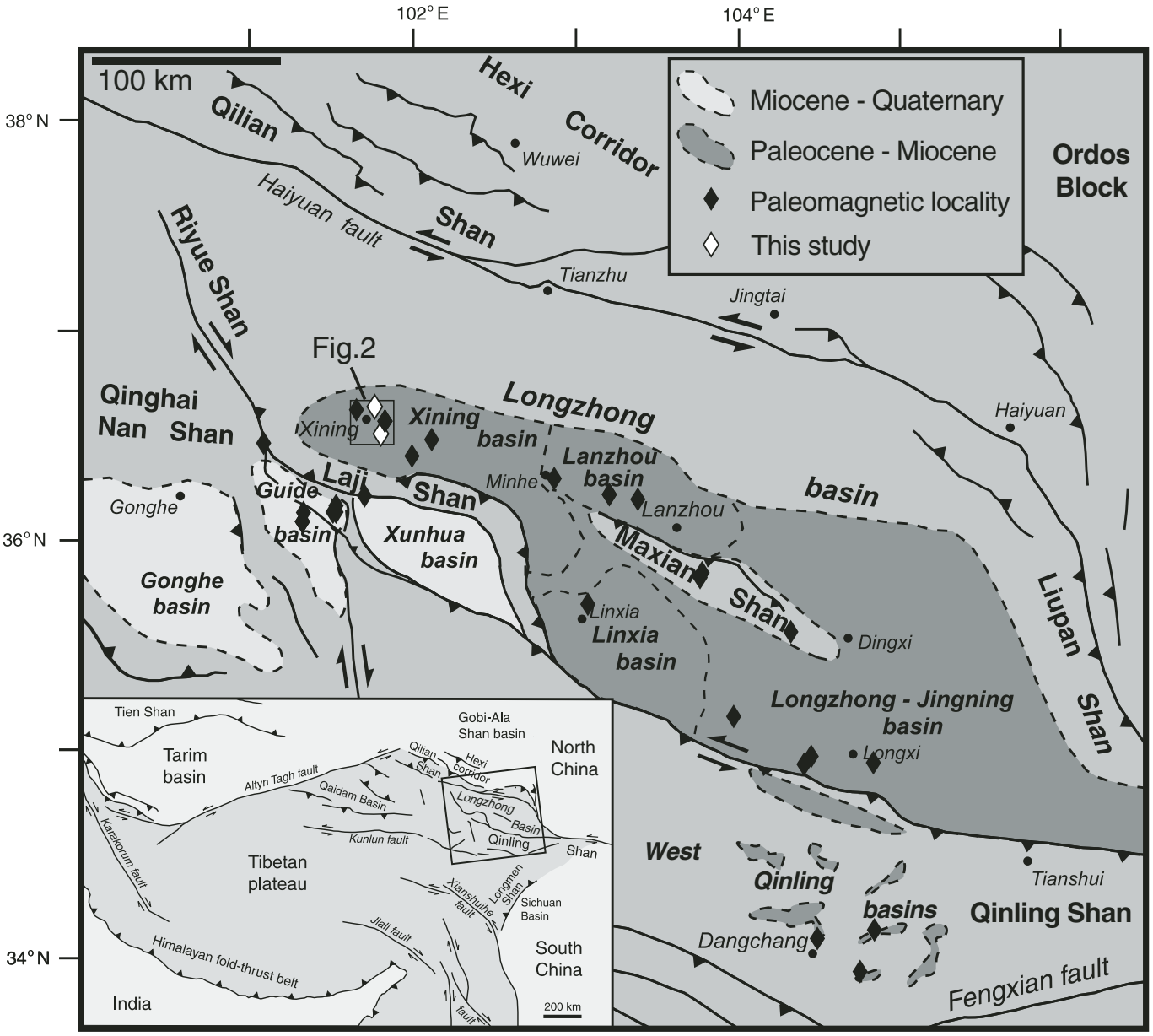

Figure 1. Simplified tectonic map of the northeastern Tibetan Plateau with approximate borders of Cenozoic basin systems (modified from Horton et al., 2004). Diamonds indicate locations of paleomagnetic sampling localities. Inset shows location in relation to the Tibetan Plateau and in the context of major tectonic features.

to relate tectonic rotations to regional geodynamics. Throughout the northeastern margin of the Tibetan Plateau, widespread clockwise tectonic rotations of ~25° have been reported (Dupont-Nivet et al., 2004; Yan et al., 2006), but the timing and geographic distribution of these rotations remain inconsistent. On the one hand, a mid-Miocene (17–11 Ma) age for the rotation is indicated in Miocene to Quaternary basins from rocks dated using magnetostratigraphy (Fang et al., 2005; Yan et al., 2006). On the other hand, an Eocene to Oligocene age has been assigned to the rotations based on previous work on rocks from Paleocene to Miocene basins (Dupont-Nivet et al., 2004). To accurately define this early phase of rotation, we provide new paleomagnetic data from the Xining Basin (Fig. 1) directly coupled to recent magnetostratigraphic dating (Dai et al., 2006). In addition, we evaluate the geographic distribution of rotations using a compilation of existing data over the northeastern Tibetan Plateau considered in a tectonic framework based on the current understanding of basin formation in the region (Horton et al., 2004).

GEOLOGIC SETTING

Two systems of Cenozoic basins are distinguished in the northeastern Tibetan Plateau (Fig. 1). The Paleocene-Miocene basin system is characterized by fining-upward sediments associated with a decreasing-upward accumulation rate (1–10 cm/k.y.) attributed to regional postrift thermal subsidence subsequent to Mesozoic extension (Horton et al., 2004). In contrast, the Miocene-Quaternary basin system is characterized by coarsening-upward sediment associated with an increasing-upward accumulation rate (20–200 cm/k.y.) in subbasins. This younger basin system is interpreted to result from progressive compartmentalization of the older larger basins by compressional and transpressional range uplift, such as the Laji Shan, which now separates the two basin systems (Horton et al., 2004; Fang et al., 2003, 2005; Pares et al., 2003).

This study was undertaken in the Xining Basin, a subbasin of the broad Longzhong Basin within the Paleocene-Miocene basin system (Figs. 1 and 2). The stratigraphic base is disconformable on the Upper Cretaceous Minhe Group. This basal discontinuity extends to the east into the adjacent Lanzhou Basin, where thicker conglomeratic series lie unconformably on folded Cretaceous rocks, suggesting post-Cretaceous tectonism east of the Xining Basin followed by regional subsidence and basin initiation or reactivation (Qiu et al., 2001; Qinghai Bureau of Geology and Mineral Resources, 1991; Zhai and Cai, 1984). Recent magnetostratigraphic dating of the particularly well-exposed, >1000-m-thick Cenozoic stratigraphy of the Xining Basin indicates subcontinuous deposition between ca. 52 Ma and 17 Ma (Dai et al., 2006; Fig. 3). The stratigraphy consists of basal sandy successions (Qijiachuan Formation, pre–52 Ma) overlain by red

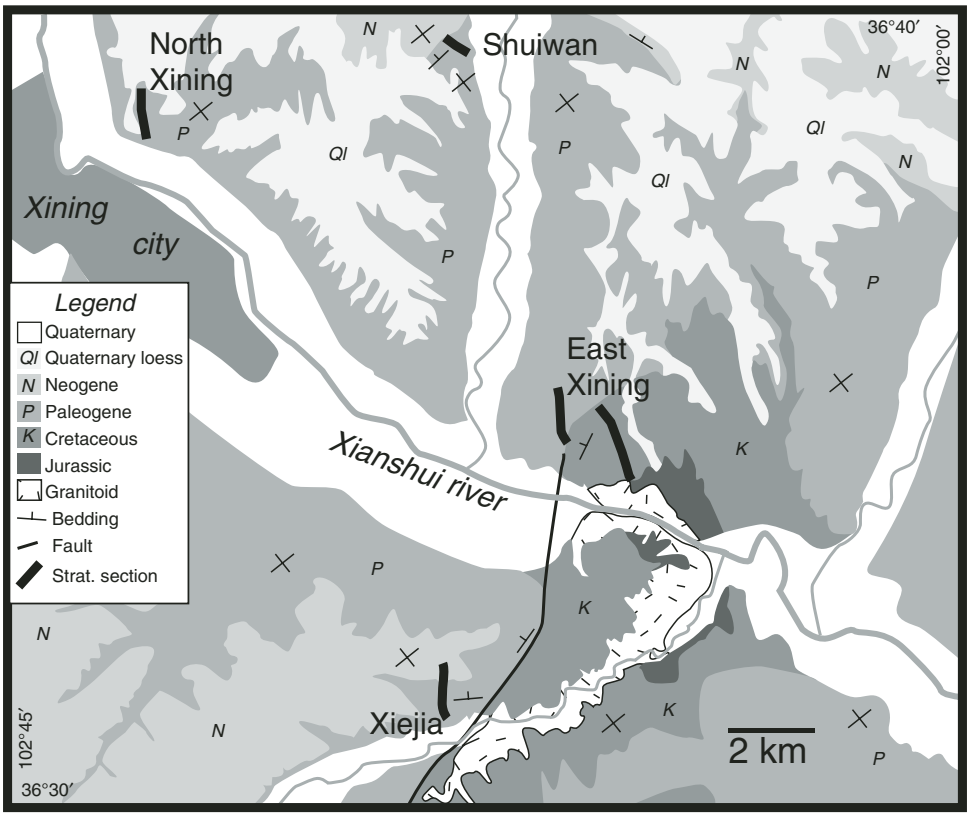

Figure 2. Geologic map of sampling locations of stratigraphic (Strat.) sections near Xining city.

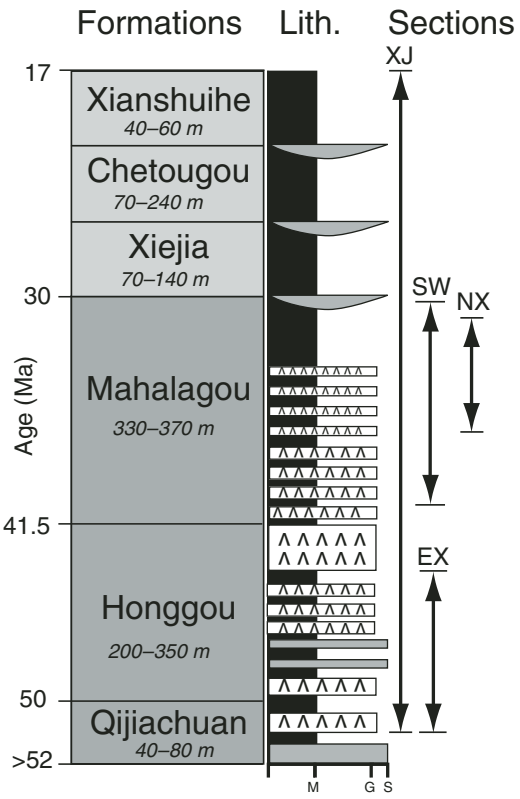

Figure 3. Generalized stratigraphic column for the Xining Basin showing formation names, ages, thickness ranges, and main lithologies (Lith.; M—mud, G—gypsum, S—sand). The sampled stratigraphic intervals are indicated within arrows for each section (XJ—Xiejia, SW—Shuiwan, NX—North Xining, EX—East Xining).

mudstones and distinctive gypsiferous intercalations (Honggou and Mahalagou Formations, 52–30 Ma) overlain by light brown to yellow mudstones with occasional sandy lenses (Xiejia, Chetougou and Xianshuihe Formations, 30–17 Ma). Apart from the disappearance of gypsum intercalations precisely correlated to the 34 Ma Eocene-Oligocene climate transition (Dupont-Nivet et al., 2007), deposition is virtually undisturbed, with slow accumulation (average 2.2 cm/k.y.) until 17 Ma, suggesting that major tectonic structures did not affect the Xining Basin until that time. Because these strata are now folded and faulted by a set of major regional E-W–trending (such as the major thrusts bounding the Laji Shan; Fig. 1) and local NW-SE–trending structures (such as the small fault and associated folding shown on Fig. 2), a post–17 Ma age is indicated for the observed deformation of the strata.

PALEOMAGNETIC SAMPLING AND ANALYSIS

Previous paleomagnetic results from the Xining Basin showed (1) ~20°–25° of clockwise rotation based on data from Cretaceous to Eocene strata up to the Honggou Formation at the East Xining section, and (2) no statistically significant rotation observed for the Oligocene Mahalagou Formation at the North Xining section (Figs. 2 and 3; Table 1; Dupont-Nivet et al., 2004). Based on these results, the timing of tectonic rotation has been estimated sometime between deposition of the Honggou Formation and the Mahalagou Formation; however, the age of these formations based on palynologic and mammalian paleontological content was only loosely constrained (Dupont-Nivet et al., 2004). Tighter age control on these formations was, however, recently provided by magnetostratigraphic studies in the Xining Basin (Dai et al., 2006). To better determine the timing of the tectonic rotations, we provide here new results from additional paleomagnetic sampling in the Xining Basin at the two following localities: (1) within the Shuiwan locality, 30 paleomagnetic sites (a paleomagnetic site is eight independently oriented samples at various stratigraphic levels within a 1–2-m-thick stratigraphic interval) were sampled throughout the Mahalagou Formation (Table 2, LJ1–LJ8 and SW1–SW22), and (2) within the Xiejia locality, 41 paleomagnetic sites were sampled throughout the Chetougou and Xianshuihe Formations (Table 2, ROT1–ROT41). These sites supplement results from magnetostratigraphic sampling of the Xiejia section throughout Xining Basin Cenozoic stratigraphy, which we also compiled here for rotational analysis (Table 3; Dai et al., 2006). Bedding attitudes were consistently measured at each site and throughout the sections, providing accurate correction of the simple homoclinal structures affecting the stratigraphy (Fig. 2).

Analysis of Paleomagnetic Sites

For samples from the Shuiwan locality, stepwise (up to 18 steps) thermal demagnetization up to 670 °C was carried out in a magnetically shielded oven, and remanence measurements were performed on a 2G 755 DC SQUID cryogenic magnetometer at the Utrecht University Paleomagnetic Laboratory. Most samples from the Shuiwan locality displayed similar demagnetization behavior; after removal of a low-temperature component below 250–350 °C, characteristic remanent magnetizations (ChRM) decay linearly, reaching the origin on vector end-point diagrams between 600 °C and 620 °C (Fig. 4A). Further linear decay until 650–670 °C displayed by a few specimens suggests the combined presence of magnetite and hematite. In some samples, overlapping of components is indicated by nonunivectorial decay displayed by a great circle path on stereographic projection. This observation suggests the presence of a partial normal overprint in some samples from the Shuiwan locality (Fig. 4A). For the samples from paleomagnetic sites at the Xiejia locality, the same treatment applied on two pilot samples at each site yielded the same general demagnetization behavior as the Shuiwan samples (Fig. 4B). The rest of the Xiejia locality samples were thus demagnetized by a combination of thermal treatment up to 350 °C to remove the contribution of possible high-coercivity phases such as goethite, followed by alternating field (AF) demagnetization (8–11 steps from 5 to 120 mT)

TABLE 1. PALEOMAGNETIC RESULTS FROM THE NORTHEASTERN TIBETAN PLATEAU

Locality/Formation	Age (Ma)	Ref.	Site location Lat. (°N)	Site location Long. (°E)	Observed direction I_s (°)	Observed direction D_s (°)	Observed direction α_{95} (°)	Observed direction *n*	Observed direction Rev. (±)	Reference pole Age (Ma)	Reference pole Lat. (°N)	Reference pole Long. (°E)	Reference pole α_{95} (°)	Rotation R (°)	±	Rotation ΔR (°)
Miocene-Quaternary Basin System																
Xunhua-Guide-Gonghe basin																
Amgigang	2.6–1.8	1	36.20	101.40	40.4	357.1	6.1	67m	+	10–0	86.3	172.0	2.6	–1.5	±	6.9
Gangjia	3.6–2.6	1	36.20	101.40	42.2	358.7	3.9	166m	+	10–0	86.3	172.0	2.6	–3.1	±	5.0
Herjia	7.8–3.6	1	36.10	101.40	42.7	3.3	1.5	635m	+	10–0	86.3	172.0	2.6	–1.1	±	3.1
Ashigong	11.5–7.8	1	36.20	101.60	44.6	4.4	3.0	157m	+	10–0	86.3	172.0	2.6	0.0	±	4.3
Low Garang	19–17.3	1	36.20	101.60	35.2	31.1	9.8	31m	+	25–15	81.4	149.7	4.5	22.5	±	10.8
Guidemen	20.8–19	1	36.20	101.60	22.5	43.9	10.4	36m	+	25–15	81.4	149.7	4.5	35.3	±	10.2
Xiongchen	N1	2	36.25	101.77	39.2	10.3	8.4	7	n/a	30–10	84.0	154.8	2.7	4.1	±	9.1
Xining	pre-N1	1	36.10	101.40	34.0	35.7	6.8	71m	+	40–20	82.8	158.1	3.8	27.9	±	7.7
Ryuieshan	K1	3	36.50	101.15	37.8	35.8	6.3	1	n/a	130–110	78.2	189.4	2.4	21.2	±	6.8
Paleocene-Miocene Basin System																
Linxia Basin																
Linxia/HWJ	6–4.3	4	35.70	103.10	40.0	3.4	5.7	67m	+	10–0	86.3	172.0	2.6	–0.9	±	6.5
Linxia/LS	7.8–6	4	35.70	103.10	34.5	9.9	6.1	51m	+	15–5	85.0	155.7	3.1	4.8	±	6.7
Linxia/DX	13.8–13.1	4	35.70	103.10	43.0	13.7	4.6	84m	+	20–10	84.2	154.9	3.2	7.8	±	6.0
Linxia/SZ	14.7–13.1	4	35.70	103.10	33.4	13.7	10.1	41m	+	20–10	84.2	154.9	3.2	7.8	±	10.2
Linxia/ZZ	21.4–14.7	4	35.70	103.10	39.5	14.6	5.0	84m	+	25–15	81.4	149.7	4.5	6.3	±	7.1
Linxia/TL	29–21.4	4	35.70	103.10	37.2	14.3	4.7	91m	+	30–20	83.8	153.2	5.3	8.1	±	7.2
Lanzhou Basin																
DuitingouU	20–15	5	36.23	103.23	38.2	8.0	4.7	100m	+	25–15	81.4	149.7	4.5	–0.4	±	6.8
DuitingouL	25–20	5	36.23	103.23	37.8	10.0	4.7	55m	+	25–15	81.4	149.7	4.5	1.6	±	6.8
Minhe	K1	3	36.30	102.90	40.4	50.5	9.8	3	n/a	130–110	78.2	189.4	2.4	35.9	±	10.6
Lanzhou	K1	3	36.20	103.40	46.9	43.2	6.8	6	n/a	130–110	78.2	189.4	2.4	28.6	±	8.3
Longzhong-Jingning Basin																
LongxiB	N2	2	34.97	104.43	56.7	4.8	5.5	5	+	10–0	86.3	172.0	2.6	0.6	±	8.4
Wenfeng	N1	2	34.94	104.80	43.7	8.8	8.5	7	n/a	30–10	84.0	154.8	2.7	2.9	±	9.8
Heichuan	E2	2	35.16	103.97	51.5	32.8	5.4	12	n/a	50–30	81.3	162.4	3.3	23.2	±	7.7
LongxiA	K1	2	34.93	104.39	40.1	47.7	6.2	6	n/a	130–110	78.2	189.4	2.4	33.3	±	6.9
Dingxi	K1	6	35.57	104.31	51.4	29.2	8.3	4	n/a	130–110	78.2	189.4	2.4	14.7	±	11.0
LintaoA	K1	6	35.85	103.78	50.3	32.3	4.2	11	+	130–110	78.2	189.4	2.4	17.7	±	5.8
LintaoB	K1	6	35.83	103.77	48.9	39.3	7.5	4	n/a	130–110	78.2	189.4	2.4	24.7	±	9.5
West Qinling basins																
NiudingShan	E1–2	2	34.18	104.81	55.3	28.5	3.1	7	n/a	60–40	80.9	164.4	3.4	18.5	±	5.6
Nanyang	E1–2	2	33.97	104.67	57.6	38.1	3.0	4	n/a	60–40	80.9	164.4	3.4	28.1	±	5.7
Dangchang	K1	2	34.08	104.47	50.9	35.8	2.9	18	n/a	130–110	78.2	189.4	2.4	21.5	±	4.4
Xining Basin																
Xiejia/Xianshuihe	18–17	*	36.52	101.87	43.3	11.6	8.6	18m	+	25–15	81.4	149.7	4.5	3.0	±	10.7
Xiejia/Xianshuihe sites	18–17	*	36.52	101.87	45.0	5.1	12.9	8	+	25–15	81.4	149.7	4.5	–3.5	±	15.5
Xiejia/Chetougou	18–23	*	36.52	101.87	41.9	8.8	6.3	55m	+	25–15	81.4	149.7	4.5	0.2	±	8.3
Xiejia/Chetougou sites	18–23	*	36.52	101.87	39.7	3.4	9.2	14	+	25–15	81.4	149.7	4.5	–5.1	±	10.8
Xiejia/Xiejia	30–23	*	36.52	101.87	51.3	3.7	3.3	162m	+	30–20	83.8	153.2	5.3	–2.6	±	7.0
Xiejia/Mahalagou	41.5–30	*	36.52	101.87	42.6	2.8	3.3	179m	+	40–30	81.2	173.4	4.6	–7.9	±	5.9
North Xining/Mahalagou	41.5–30	2	36.65	101.78	40.2	12.8	5.3	17	+	40–30	81.2	173.4	4.6	2.0	±	7.3
Xiejia/Honggou	50–41.5	*	36.52	101.87	40.1	26.2	5.6	33m	+	50–40	81.1	150.4	5.3	17.2	±	8.2
East Xining/Honggou	50–41.5	2	36.58	101.89	33.7	26.8	11.9	9	+	50–40	81.1	150.4	5.3	17.8	±	12.8
Xining/Honggou	50–41.5	7	36.5	102.0	40.8	29.3	13.2	5	i	50–40	81.1	150.4	5.3	20.3	±	15.2
Shancheng/Minhe	K2	2	36.38	102.05	33.9	30.1	9.6	15	n/a	90–70	81.4	206.1	5.9	20.0	±	10.9
East Xining/Hekou	K1	2	36.58	101.89	33.6	37.7	4.5	20	+	130–110	78.2	189.4	2.4	23.0	±	4.9

Note: Locality/Formation—paleomagnetic locality and sampled formation; Age—age of sampled formation given by numbers when magnetostratigraphic control on age span is available or given by epoch notation otherwise (K1—Early Cretaceous; K2—Late Cretaceous; E1—Paleocene; E2—Eocene; E3—Oligocene; N1—Miocene; N2—Pliocene). Lat. and Long.—latitude and longitude; Is and Ds—inclination and declination in stratigraphic coordinates; α_{95}—angular radius of 95% confidence on mean direction; *n*—number of sites used to calculate mean direction (followed by "m" if number of characteristic remanent magnetization (ChRM) directions from magnetostratigraphic levels); Rev.—outcome of reversals test ("+" if positive, "i" if indeterminate, and "n/a" if not applicable); Reference pole—Eurasian paleomagnetic pole from Besse and Courtillot (2002); Age—pole age limits of average sliding window; α_{95}—pole 95% confidence limit; R—vertical-axis rotation (clockwise is positive); ΔR—95% confidence limit on R; Rotation and flattening are derived from observed direction minus expected direction at locality calculated from reference pole.

References (Ref.): *—this study; 1—Yan et al. (2006); 2—Dupont-Nivet et al. (2004); 3—Halim et al. (1998); 4—Fang et al. (2003); 5—Flynn et al. (1999); 6—Yang et al. (2002); 7—Cogné et al. (1999).

TABLE 2. PALEOMAGNETIC SITE-MEAN DIRECTIONS

Site ID#	Level (m)	*n*	Dg (°)	Ig (°)	Ds (°)	Is (°)	*k*	α_{95} (°)
Shuiwan locality								
Mahalagou Formation								
LJ001*	<–10	7	25.9	45.0	23.5	43.3	17.3	14.9
LJ002	<–10	11	12.2	43.6	10.3	41.3	168.6	3.5
LJ003	<–10	8	27.7	29.3	26.4	27.7	29.5	10.4
LJ005*	<–10	4	211.3	–38.6	210.1	–38.1	36.4	15.4
LJ006*	<–10	7	227.8	–28.9	226.2	–28.2	12.6	17.7
LJ008*	<–10	8	224.4	–34.8	222.9	–34.1	19.2	13.0
SW001*	–10	8	135.7	–45.6	139.9	–16.3	27.0	10.9
SW002	–11	5	225.0	–25.1	214.8	–14.0	48.5	11.1
SW003*	–12	4	217.4	–44.5	198.6	–27.7	15.0	24.6
SW004*	–15	8	208.6	–51.9	188.5	–31.1	16.3	14.2
SW005	–16	8	233.9	–37.9	214.4	–28.9	90.6	5.9
SW006	–17	5	272.5	–56.9	220.8	–60.2	44.9	11.5
SW007*	–20	7	241.5	–34.7	222.3	–29.8	18.5	14.4
SW008*	–21	8	229.1	–44.8	206.4	–32.5	9.8	18.6
SW009*	–23	4	263.6	–60.5	210.2	–58.0	20.5	20.8
SW010*	–25	3	321.0	–60.4	232.1	–85.0	1.2	99.9
SW011	11	6	36.6	43.4	18.6	26.4	179.3	5.0
SW012	15	7	20.0	53.5	2.2	30.1	43.8	9.2
SW013	18	8	34.7	43.6	17.2	25.9	54.5	7.6
SW014*	55	8	40.8	47.8	18.8	31.7	12.3	16.5
SW015	74	8	53.1	47.7	27.0	36.5	34.0	9.6
SW016	78	6	235.9	–39.5	214.8	–31.1	25.9	13.4
SW017*	82	4	16.3	57.3	358.1	32.6	20.8	20.6
SW018	84	5	235.2	–67.6	188.4	–51.4	29.6	14.3
SW019*	88	7	274.2	–57.4	220.8	–61.3	5.8	27.4
SW020*	101	8	249.1	–52.5	212.9	–46.9	9.6	18.8
SW021*	105	6	260.2	–68.7	194.4	–60.1	15.2	17.7
SW022*	114	4	273.2	–55.9	222.9	–60.1	22.5	19.8
Shuiwan geographic		11	42.6	46.0			18.9	10.8
Shuiwan stratigraphic		11			23.1	34.4	24.8	9.4
Shuiwan normal		6			17.0	31.6	63.0	8.5
Shuiwan reverse		5			211.3	–37.5	15.7	19.9
Indeterminate reversals test; critical angle = 21.2°; normal/reverse angle = 13.2°.								
Xiejia locality								
Xianshuihe Formation								
ROT27	782	8	17.5	53.6	9.8	50.1	160.9	4.4
ROT28	784	8	189.5	–53.3	182.6	–49.0	153.1	4.5
ROT30	789	5	20.4	24.3	17.7	21.3	40.5	12.2
ROT31	793	5	44.6	32.7	40.1	32.5	31.8	13.8
ROT32	798	8	183.3	–63.5	174.4	–58.5	166.5	4.3
ROT33	800	8	186.6	–54.1	179.8	–49.5	33.2	9.8
ROT34–37*	810	7	178.6	–49.0	173.7	–43.8	17.2	15.0
ROT39	818	7	343.3	47.0	340.2	40.8	143.0	5.1
ROT41	825	6	169.8	–50.9	165.5	–45.1	57.4	8.9
Xianshuihe geographic		8	11.2	49.1			19.4	12.9
Xianshuihe stratigraphic		8			5.1	45.0	19.4	12.9
Chetougou Formation								
ROT1	780	8	38.8	32.9	34.4	32.0	83.5	6.1
ROT10*	748	8	352.6	39.0	349.5	33.4	19.5	12.9
ROT11	747	7	355.1	27.1	353.1	21.7	41.1	9.5
ROT13*	705	5	193.3	–48.9	187.1	–45.0	15.3	20.2
ROT14	704	5	201.5	–48.7	194.7	–45.6	56.9	10.2
ROT16	700	7	210.1	–43.9	203.9	–41.8	27.8	11.6
ROT17	697	6	206.5	–42.0	200.8	–39.6	30.1	12.4
ROT19	683	7	184.6	–39.3	180.6	–34.7	75.3	7.0
ROT2	779	6	31.0	64.8	17.7	62.4	352.2	3.6
ROT20	680	8	166.5	–50.6	162.6	–44.6	78.6	6.3
ROT22	677	6	170.5	–25.0	168.8	–19.3	28.6	12.7
ROT24	671	8	204.7	–50.8	197.2	–48.0	47.7	8.1
ROT25	669	8	353.8	46.6	349.7	41.1	30.3	10.2
ROT4	776	3	20.0	50.1	13.0	46.9	135.4	10.6
ROT5	774	6	356.4	27.8	354.2	22.5	25.9	13.4
ROT6	766	7	333.2	43.4	331.4	36.8	47.9	8.8

(*continued*)

TABLE 2. PALEOMAGNETIC SITE-MEAN DIRECTIONS (*continued*)

Site ID#	Level (m)	*n*	Dg (°)	Ig (°)	Ds (°)	Is (°)	*k*	α_{95} (°)
Chetougou geographic		14	8.4	44.0			19.5	9.2
Chetougou stratigraphic		14			3.4	39.7	19.5	9.2
Xiejia sites normal		11			5.2	39.0	14.2	12.6
Xiejia sites reverse		11			182.7	–44.2	31.2	8.3
Positive reversals test class C; critical angle = 15.1°; normal/reverse angle = 5.5°.								

Note: Site ID#—paleomagnetic site identification; Ig and Dg—inclination and declination of site-mean direction in geographic coordinates (with no structural correction); Is and Ds—inclination and declination of site-mean direction in stratigraphic coordinates (after restoration of local bedding to horizontal); *k*—concentration parameter; α_{95}—angular radius of 95% confidence on mean direction; *n*—number of sample characteristic remanent magnetization (ChRM) directions averaged to calculate site-mean direction. Averages of site-mean directions are given by formation and by polarity (normal and reverse); reversals test—outcome of the reversals test of McFadden and McElhinny (1990).
*Discarded site-mean direction.

TABLE 3. FORMATION-MEAN DIRECTIONS FROM XIEJIA MAGNETOSTRATIGRAPHIC SECTION (DAI ET AL., 2006)

Formation	*n*	Dg (°)	Ig (°)	Ds (°)	Is (°)	*k*	α_{95} (°)
Xianshuihe geographic	18	19.2	48.4			15.1	9.2
Xianshuihe stratigraphic	18			11.6	43.3	17.1	8.6
Xianshuihe normal	5			24.5	42.9	38.8	12.4
Xianshuihe reverse	13			186.5	–43.1	15.0	11.1
Positive reversals test class C; critical angle = 15.9°; normal/reverse angle = 13.2°.							
Cwhetougou geographic	55	16.7	49.8			14.0	5.3
Chetougou stratigraphic	55			8.8	41.9	17.3	6.3
Chetougou normal	32			7.2	41.7	15.9	6.5
Chetougou reverse	23			191.9	–52.0	11.4	9.4
Positive reversals test class C; critical angle = 11.2°; normal/reverse angle = 10.8°.							
Xiejia geographic	162	22.9	54.6			12.1	3.3
Xiejia stratigraphic	162			3.7	51.3	12.1	3.3
Xiejia normal	75			4.1	50.2	12.6	4.8
Xiejia reverse	87			183.4	–52.2	11.6	4.7
Positive reversals test class B; critical angle = 6.6°; normal/reverse angle = 2.1°.							
Mahalagou geographic	179	64.2	44.1			10.1	3.5
Mahalagou stratigraphic	179			2.8	42.6	11.1	3.3
Mahalagou normal	55			359.4	41.5	12.5	5.7
Mahalagou reverse	124			184.4	–43.0	10.1	4.6
Positive reversals test class B; critical angle = 9.1°; normal/reverse angle = 4.0°.							
Honggou geographic	33	58.7	33.1			16.3	6.4
Honggou stratigraphic	33			26.2	40.1	21.2	5.6
Honggou normal	19			20.5	41.5	25.2	6.8
Honggou reverse	14			213.8	–37.8	19.8	9.2
Positive reversals test class C; critical angle = 11.2°; normal/reverse angle = 10.9°.							
Qijiachuan geographic	17	53.3	45.9			8.2	13.2
Qijiachuan stratigraphic	17			5.7	47.3	13.3	10.2
Qijiachuan normal	13			356.1	48.7	15.6	10.9
Qijiachuan reverse	4			211.9	–38.5	30.9	16.8
Negative reversals test; critical angle = 20.8°; normal/reverse angle = 27.5°.							

Note: Formation—name of formation over which characteristic remanent magnetization (ChRM) directions have been averaged. Ig and Dg—inclination and declination of formation-mean direction in geographic coordinates (with no structural correction); Is and Ds—inclination and declination of formation-mean direction in stratigraphic coordinates (after restoration of local bedding to horizontal); *k*—concentration parameter; α_{95}—radius of cone of 95% confidence about formation-mean direction; *n*—number of sample ChRM directions averaged to calculate formation-mean paleomagnetic direction. Average directions are also given for normal and reverse polarity within each formation. Reversals test—outcome of the application of the reversals test of McFadden and McElhinny (1990).

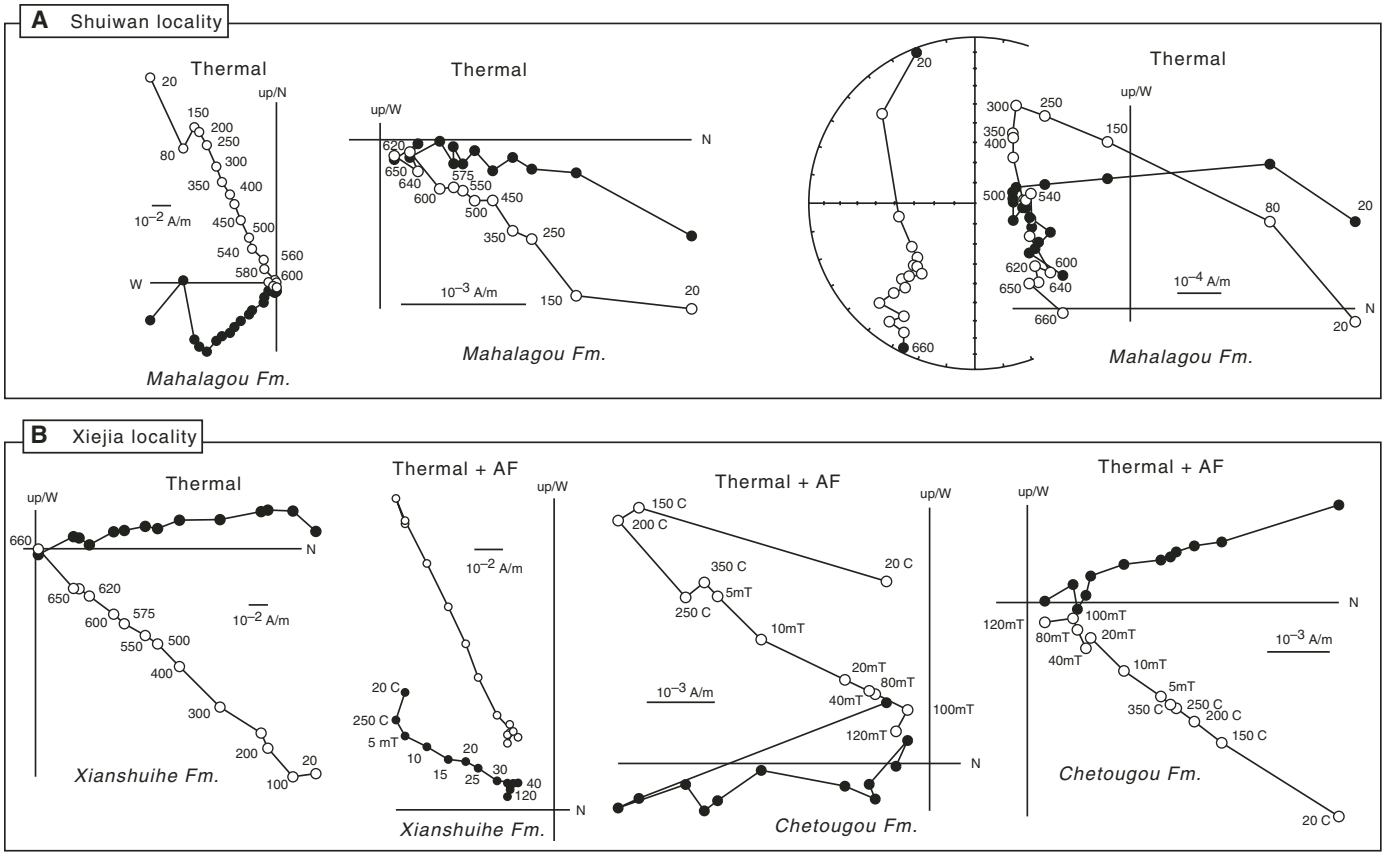

Figure 4. Characteristic vector end-point diagrams of demagnetizations. (A) Thermal demagnetization of the Shuiwan locality in the Mahalagou Formation. Right-side diagram shows overlapping components interpreted to result from partial normal overprint. (B) Thermal and alternating field (AF) demagnetizations of the Xiejia locality in the Xianshuihe and Chetougou Formations. Projection in the horizontal (vertical) plane is illustrated by black (open) dots, and adjacent numbers correspond to temperature step in °C or peak AF in mT.

using an inline 2G degausser and RF-SQUID magnetometer with sample autofeeder in a shielded room. For most samples, this AF treatment successfully demagnetized 80%–100% of the ChRM, further suggesting magnetite as the dominant carrier. All ChRM directions were assessed on vector end-point diagrams and calculated using least squares analysis (Kirschvink, 1980) to estimate the maximum angular deviation (MAD) on a minimum of four measurements. These principal component analyses were performed without forcing line fits through the origin. A few samples showing erratic demagnetization behavior resulting in ChRM directions with a MAD above 15° were systematically rejected. The remaining ChRM directions used in this analysis have straightforward demagnetization behavior and low MAD values, typically 10° to 5° (Fig. 4). On the remaining ChRM directions, Fisher (1953) statistics were used to calculate site-mean directions and their α_{95} (95% confidence angle) from the paleomagnetic sites at both localities (Table 2). To avoid any possible bias from isolated outlying directions, site-mean directions with α_{95} above 15° and/or dispersion parameter (k) below 20 were systematically rejected for further analysis, as well as one widely aberrant direction (SW001) from the Shuiwan section data set. After structural corrections, the remaining site-mean directions were compared on stereographic projections showing separate sets of normal- and reversed-polarity directions (Fig. 5).

Analysis of Magnetostratigraphic ChRM Directions

For rock magnetic analysis of magnetostratigraphic levels from the Xiejia section, see Dai et al. (2006). Of the ChRM directions reported in Dai et al. (2006), all directions with MAD above 15° were systematically rejected for the present analysis. In addition, to remove possible transitional directions likely found in these sediments, where low sedimentation rates record a relatively high of number of paleomagnetic reversals, we applied the recursive cut-off method developed by Vandamme (1994) on separate sets of reverse- and normal-polarity populations from each formation. On the remaining ChRM directions, Fisher (1953) statistics were used to calculate formation-mean directions for the formations sampled for magnetostratigraphy at the Xiejia section (Table 3). After structural corrections, the remaining ChRM directions were compared on stereographic projections showing separate sets of normal- and reversed-polarity directions (Fig. 6).

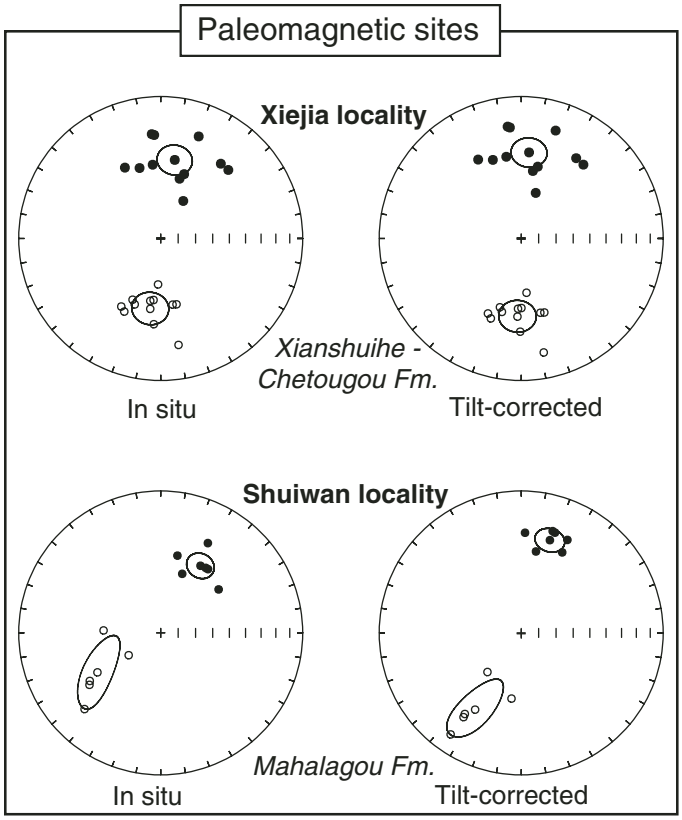

Figure 5. Stereographic projections in the lower (black dots) and upper (open dots) hemisphere of site-mean directions from the Xiejia and Shuiwan localities given before (in situ) and after (tilt corrected) tilt corrections. Averages of normal and reverse site-mean directions are given with 95% confidence ellipse (Tauxe, 1998).

PALEOMAGNETIC RESULTS

Reliability Tests

Although prefolding magnetization is indicated by a positive regional fold test (McFadden, 1990) applied to the combined site-mean directions and formation-mean directions, the reversals test of McFadden and McElhinny (1990) yielded mixed results and shed light on the primary origin and the reliability of the observed directions critical for rotational analysis. The reversals test applied to site-mean directions was positive for the Xiejia locality sites but indeterminate for the Shuiwan locality

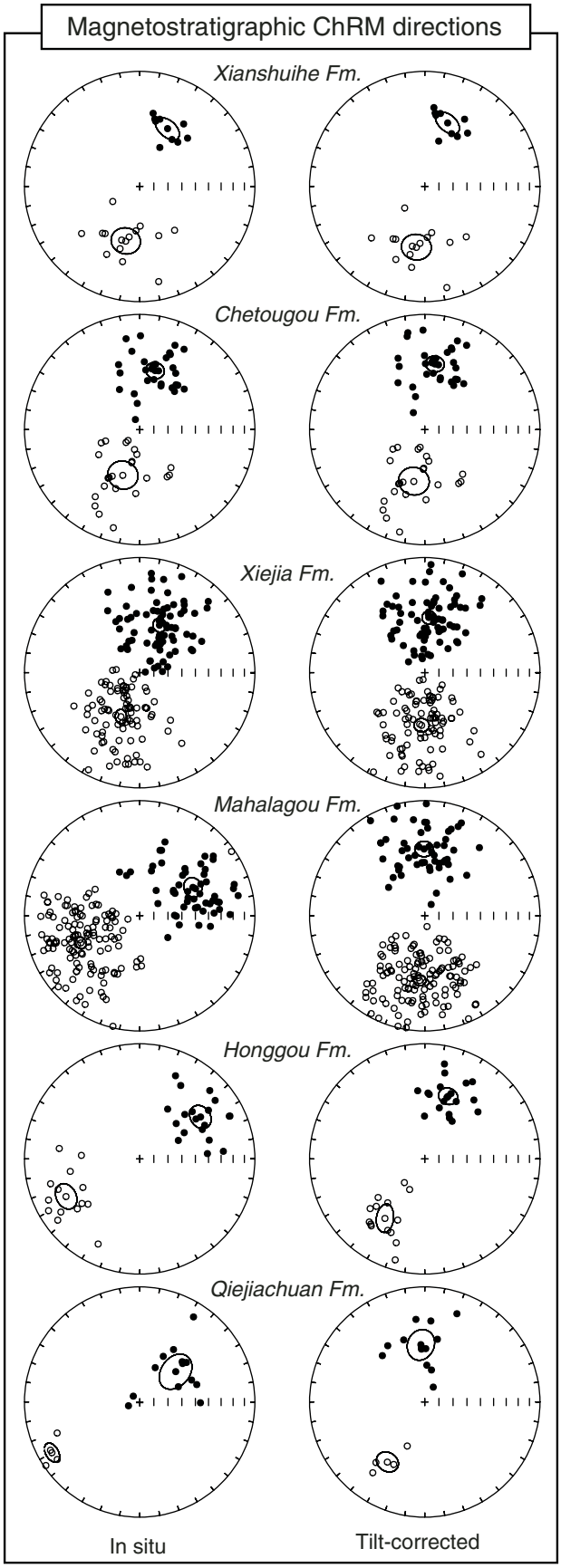

Figure 6. Stereographic projections in the lower (black dots) and upper (open dots) hemisphere of characteristic remanent magnetization (ChRM) directions from the magnetostratigraphy of different formations at the Xiejia section given before (in situ) and after (tilt corrected) tilt corrections. Averages of normal and reverse site-mean directions are given with 95% confidence ellipse (Tauxe, 1998).

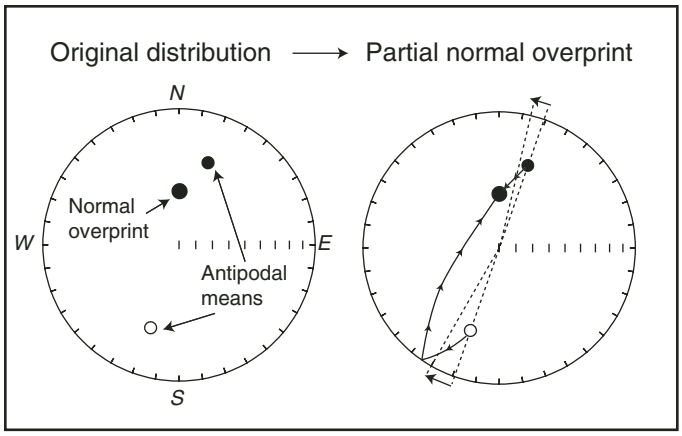

Figure 7. Illustration of the potential effect of an unresolved partial normal overprint on an originally antipodal distribution (left plot). The mean normal direction is biased toward a steeper and more northerly direction, while the mean reversed direction is biased toward a shallower and more westerly direction (right plot).

sites (Table 2). For magnetostratigraphic results from the Xiejia sections, the reversals test was applied to ChRM directions for each formation. All passed the reversals test, except for ChRM of the Qijiachuan Formation (Table 3). For both data sets that failed the reversals test, a clear bias of normal directions toward more northerly direction and reversed direction toward more westerly directions was observed. Based on this characteristic distribution of site-mean directions, we interpret the failure of the reversals test for these data sets to result from the partial contribution of an unresolved normal-polarity overprint as illustrated on Figure 7. Failure of the reversals test for these two data sets reflects a significant bias in directions that preclude using them for analysis of tectonic rotation. As a result, we rejected these two data sets from further analysis. For the remaining data sets from the Honggou to Xianshuihe Formations, positive reversals tests with nearly antipodal normal and reverse directions suggest that these directions have not been significantly biased, and thus they provide a set of reliable results for rotational analysis.

TABLE 4. INCREMENTAL MOVING AVERAGE OVER MAGNETOSTRATIGRAPHIC ChRM DIRECTIONS

Level (m)	*n*	Dm (°)	Im (°)	*k* (°)	α_{95} (°)	Age (Ma)	Dx (°)	±	δD (°)	R (°)	±	ΔR (°)
367.5	15	0.5	48.4	12.9	11.1	34.13	10.0	±	4.3	–9.4	±	13.9
364.6	15	2.5	49.0	11.9	11.6	34.20	10.0	±	4.3	–7.5	±	14.6
361.6	15	4.4	46.6	13.3	10.9	34.26	10.0	±	4.3	–5.6	±	13.2
358.5	15	5.3	47.3	14.5	10.4	34.33	10.0	±	4.3	–4.7	±	12.8
355.7	15	5.1	46.6	13.8	10.7	34.39	10.0	±	4.3	–4.8	±	13.0
353.0	15	5.6	43.3	13.0	11.0	34.45	10.0	±	4.3	–4.3	±	12.7
350.1	15	3.3	43.2	14.5	10.4	34.51	10.0	±	4.3	–6.6	±	12.0
347.8	15	2.0	42.2	13.5	10.8	34.56	10.0	±	4.3	–7.9	±	12.2
345.6	15	2.8	41.4	13.9	10.6	34.61	10.0	±	4.3	–7.2	±	11.9
343.9	15	1.3	40.0	12.6	11.2	34.64	10.0	±	4.3	–8.7	±	12.3
342.1	15	1.2	36.9	12.8	11.1	34.75	10.0	±	4.3	–8.7	±	11.7
340.0	15	2.8	37.2	12.5	11.2	34.90	10.0	±	4.3	–7.2	±	11.9
338.0	15	5.5	38.5	12.8	11.1	35.06	10.0	±	4.3	–4.5	±	11.9
336.0	15	5.6	39.0	12.7	11.2	35.21	10.0	±	4.3	–4.4	±	12.1
333.8	15	3.2	35.6	10.9	12.1	35.37	10.0	±	4.3	–6.7	±	12.5
331.8	15	2.6	32.7	11.2	12.0	35.54	10.0	±	4.3	–7.3	±	11.9
329.5	15	0.7	32.0	12.7	11.2	35.72	10.0	±	4.3	–9.2	±	11.1
327.2	15	–1.6	33.4	11.0	12.1	35.91	10.0	±	4.3	–11.5	±	12.1
324.6	15	0.6	34.0	10.7	12.3	36.13	10.0	±	4.3	–9.4	±	12.4
322.0	15	–3.3	33.0	9.5	13.1	36.34	10.0	±	4.3	–13.2	±	13.0
319.6	15	–2.0	34.0	8.9	13.6	36.57	10.0	±	4.3	–11.9	±	13.6
317.2	15	–4.3	36.0	8.5	13.9	36.74	10.0	±	4.3	–14.3	±	14.3
314.6	15	–0.5	37.9	8.1	14.3	36.90	10.0	±	4.3	–10.4	±	15.0
312.0	15	–0.7	38.4	8.0	14.4	37.07	10.0	±	4.3	–10.7	±	15.2
309.1	15	2.4	39.5	8.6	13.8	37.26	10.0	±	4.3	–7.5	±	14.9
306.1	15	–0.6	41.7	9.3	13.2	37.45	10.0	±	4.3	–10.5	±	14.7
303.2	15	–4.8	42.3	9.6	13.0	37.63	10.0	±	4.3	–14.8	±	14.6
300.3	15	–8.2	40.4	9.4	13.2	37.82	10.0	±	4.3	–18.2	±	14.4
297.4	15	–6.4	38.2	9.2	13.3	38.00	10.0	±	4.3	–16.3	±	14.1
294.6	15	–5.1	39.4	10.2	12.6	38.16	10.0	±	4.3	–15.0	±	13.5
291.7	15	–5.1	41.9	10.7	12.3	38.26	10.0	±	4.3	–15.1	±	13.7
288.5	15	–4.6	42.3	10.5	12.4	38.38	10.0	±	4.3	–14.6	±	13.9
285.2	15	–1.8	43.3	10.1	12.7	38.52	10.0	±	4.3	–11.7	±	14.5
282.3	15	–1.3	42.7	9.9	12.8	38.66	10.0	±	4.3	–11.2	±	14.4
279.3	15	2.2	47.5	10.9	12.2	38.81	10.0	±	4.3	–7.8	±	14.9
276.3	15	1.7	49.1	11.5	11.8	38.95	10.0	±	4.3	–8.3	±	14.9
272.5	15	6.7	49.0	11.1	12.0	39.13	10.0	±	4.3	–3.3	±	15.2
268.8	15	4.8	50.5	10.3	12.5	39.31	10.0	±	4.3	–5.2	±	16.3
264.9	15	5.5	50.1	10.1	12.6	39.49	10.0	±	4.3	–4.4	±	16.3

(*continued*)

Rotational Analysis

Based on the data sets accepted by the reliability tests, we examined the likelihood of vertical-axis rotation during deposition of sediments. When comparing results by formations, a marked decrease in declination is immediately apparent between the Honggou Formation, which has N-NE declination, and the Mahalagou and subsequent formations, which show northerly declinations (Fig. 6). To estimate this decrease in rotation, the net rotation values are formally derived following the methods of Beck (1980) and Demarest (1983) by comparing formation means to the expected direction calculated using the reference paleomagnetic pole for Eurasia (Besse and Courtillot, 2002) of the appropriate age (Table 1). This analysis suggests that a net clockwise rotation of ~20°, significant at the 95% confidence level, occurred sometime between deposition of the Honggou and Mahalagou Formations, as previously observed in published results from the Xining Basin (Dupont-Nivet et al., 2004). We note that inclination values are systematically lower than the ~60° expected from the apparent polar wander path of Eurasia of this age. This can be interpreted as resulting from flattening of inclination during depositional processes and subsequent compaction as observed in numerous red beds in Asia (Dupont-Nivet et al., 2002b; Gilder et al., 2001).

To better estimate the timing of the rotation, we focus on the declination values between the Honggou and Mahalagou Formations from the available magnetostratigraphic ChRM direction data set of the Xiejia section. The age of magnetostratigraphic levels is estimated by linear interpolation of assumed constant accumulation rate to the nearest correlated chron boundary (Dai et al., 2006). Throughout these formations from 34 to 48 Ma, we applied a sliding window, averaging Fisher (1953) statistics for 15 successive ChRM directions incrementally at each ChRM direction (Table 4). These moving averages of 15 ChRM directions included long time spans from the magnetostratigraphic data set (longer than 2 m.y.), likely averaging paleosecular

TABLE 4. INCREMENTAL MOVING AVERAGE OVER MAGNETOSTRATIGRAPHIC ChRM DIRECTIONS (*continued*)

Level (m)	*n*	Dm (°)	Im (°)	*k* (°)	α_{95} (°)	Age (Ma)	Dx (°)	±	δD (°)	R (°)	±	ΔR (°)
259.7	15	5.2	49.9	10.1	12.7	39.74	10.0	±	4.3	–4.8	±	16.3
254.4	15	8.4	50.6	10.1	12.7	40.00	10.0	±	4.3	–1.6	±	16.5
249.6	15	12.4	51.8	11.8	11.6	40.26	10.0	±	4.3	2.5	±	15.6
244.9	15	19.0	51.5	13.8	10.7	40.58	10.0	±	4.3	9.0	±	14.3
240.2	15	21.9	51.8	15.0	10.2	40.88	10.0	±	4.3	11.9	±	13.8
235.5	15	25.2	54.0	19.0	9.0	41.20	10.0	±	4.3	15.2	±	12.8
230.6	15	28.2	54.8	19.9	8.8	41.52	10.0	±	4.3	18.3	±	12.8
226.2	15	30.9	52.7	17.8	9.3	41.81	10.0	±	4.3	20.9	±	12.9
221.5	15	30.4	50.6	18.8	9.1	42.12	10.0	±	4.3	20.5	±	12.0
216.7	15	30.4	50.1	18.0	9.3	42.44	10.0	±	4.3	20.5	±	12.1
211.9	15	31.1	48.0	22.0	8.3	42.84	10.0	±	4.3	21.2	±	10.6
206.9	15	29.2	47.8	22.3	8.3	43.28	10.0	±	4.3	19.2	±	10.5
202.1	15	27.1	46.1	20.2	8.7	43.71	10.0	±	4.3	17.2	±	10.7
196.8	15	29.1	43.2	27.6	7.4	44.00	10.0	±	4.3	19.2	±	8.9
191.2	15	29.9	41.7	25.5	7.7	44.27	10.0	±	4.3	19.9	±	9.0
187.4	15	32.9	41.8	27.0	7.5	44.45	10.6	±	4.5	22.3	±	8.8
183.6	15	32.7	42.4	24.3	7.9	44.63	10.6	±	4.5	22.1	±	9.3
179.6	15	33.4	42.5	24.9	7.8	44.82	10.6	±	4.5	22.8	±	9.2
175.4	15	30.3	43.4	21.1	8.5	45.02	10.6	±	4.5	19.7	±	10.1
170.8	15	29.7	44.5	22.5	8.2	45.24	10.6	±	4.5	19.1	±	9.9
166.3	15	27.7	41.9	19.3	8.9	45.46	10.6	±	4.5	17.1	±	10.3
161.9	15	26.1	39.0	21.1	8.5	45.67	10.6	±	4.5	15.5	±	9.5
157.3	15	23.7	41.2	19.8	8.8	45.89	10.6	±	4.5	13.1	±	10.1
152.6	15	23.0	39.1	16.4	9.7	46.11	10.6	±	4.5	12.4	±	10.7
146.9	15	24.4	40.0	15.9	9.9	46.45	10.6	±	4.5	13.8	±	11.0
141.1	15	24.7	38.5	15.7	10.0	46.85	10.6	±	4.5	14.1	±	10.8
135.0	15	25.4	38.2	15.8	9.9	47.28	10.6	±	4.5	14.8	±	10.7
129.7	15	27.5	39.3	15.7	10.0	47.65	10.6	±	4.5	16.9	±	10.9
124.8	15	26.4	38.2	15.7	10.0	47.95	10.6	±	4.5	15.8	±	10.8

Note: Level—average stratigraphic level in meters according to levels given in Dai et al. (2006); *n*—number of characteristic remanent magnetization (ChRM) directions averaged (fixed to 15); Im and Dm—Fisher (1953) statistic mean inclination and declination of 15 ChRM directions within sliding window (in stratigraphic coordinates); *k*—concentration parameter; α_{95}— radius of cone of 95% confidence about mean direction; Age—age of the average stratigraphic level estimated using linear interpolation to the nearest correlated chron (Dai et al., 2006); $D_x \pm \delta D$—expected declination and associated 95% confidence calculated from the apparent polar wander path of Besse and Courtillot (2002) of Eurasia at 40 and 50 Ma; $R \pm \Delta R$—rotation and associated 95% confidence derived following the methods of Beck (1980) and Demarest (1983).

variation. This procedure yielded window-mean directions with 95% confidence angles ranging from 7.4° to 14.4° (average = 10.9°). To estimate the timing of the rotation, the obtained window-mean declinations were plotted with respect to their magnetostratigraphically determined age averaged over the sliding window and compared to the expected declination calculated from the apparent polar wander path (Fig. 8). The record of clockwise rotation is clearly indicated by a progressive decrease in declinations occurring at ca. 41 Ma, in the lower part of the Mahalagou Formation. On either side of the transition, the nearest statistically different window-mean directions are found at 41.8 Ma (declination of 30.9° ± 9.3°) and 39.7 Ma (declination of 5.2° ± 12.9°), respectively, and most of the declination decrease is recorded within this time interval. In addition, the rotation (defined as the difference between the observed and expected declination; see Table 4) is statistically significant at 41.8 Ma (rotation of 20.9° ± 12.9°) and decreases systematically until 39.7 Ma, when it becomes insignificant (rotation of –4.8° ± 16.3°). As a result, we interpret the rotation to have occurred ca. 41 Ma, mostly between 41.8 Ma and 39.7 Ma.

DISCUSSION

Diachronous Rotations in Two Basin Systems

To understand the regional significance of our results, we examined existing paleomagnetic data over the northeastern Tibetan Plateau region (Table 1). Consistent with our results, previous studies from the Xining Basin show clockwise rotations of ~20°–30° in sediments from the Honggou Formation and older rocks, and no statistically significant rotations in younger deposits (Dupont-Nivet et al., 2004, Cogné et al., 1999). More regionally, data from the rest of the Paleocene-Miocene basin system are consistent in magnitude and timing with Xining Basin rotations (Fig. 9A). Clockwise rotations of ~15°–35° are systematically recorded in Paleogene and older rocks, and no significant rotation since at least 29 Ma is recorded by magnetostratigraphically dated sediments from the Linxia Basin (Fang et al., 2003). The sum of these results indicates that a regional tectonic mechanism generating widespread clockwise rotations was active during the early history of the Paleocene-Miocene basin system. Remarkably, the existing paleomagnetic data from the Gonghe-Guide-Xunhua basins (Fang et al., 2005; Yan et al., 2006) show a mid-Miocene (17–11 Ma) ~25° clockwise rotation that is restricted to the Miocene-Quaternary basin system located to the west of the Laji Shan range (except for the poorly dated Xiongchen locality; see Fig. 9B). The fact that this second rotation phase does not appear to have affected the Paleogene-Miocene basin system suggests a mid-Miocene regional westward shift of deformation and tectonic activity on the structural boundary between the two basin systems (i.e., the Laji Shan thrust belt; Fig. 1) during the mid-Miocene between ca. 17 and 11 Ma.

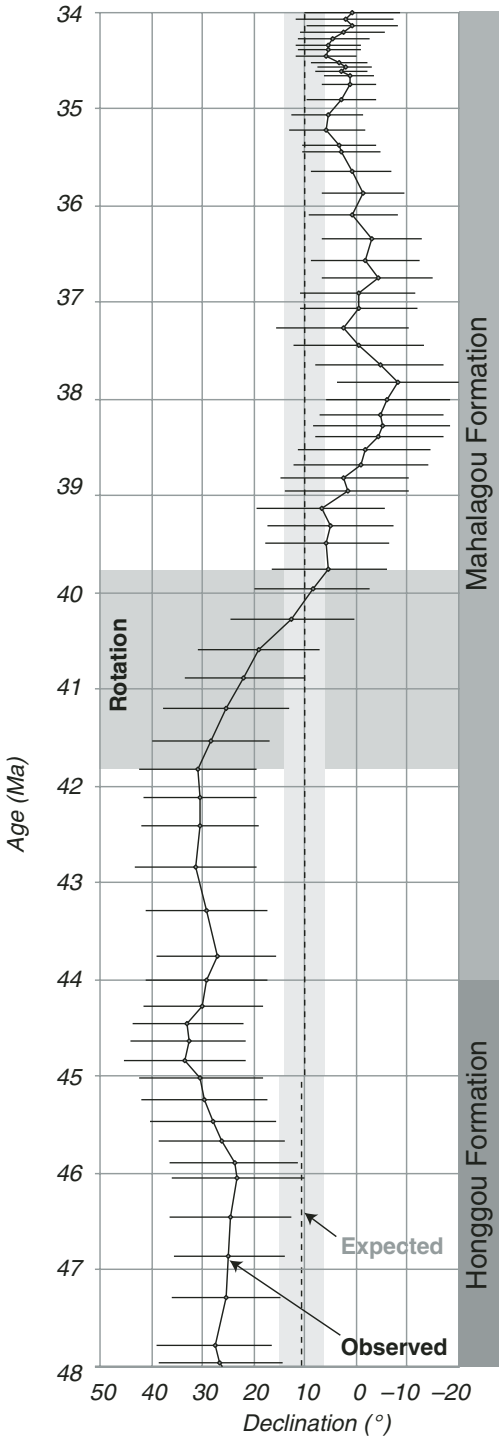

Figure 8. Moving average over the magnetostratigraphic characteristic remanent magnetization (ChRM) directions of the Xiejia section from 34 to 48 Ma (Dai et al., 2006). A sliding window was applied, averaging Fisher (1953) statistics for 15 successive ChRM directions incrementally at each ChRM direction (see Table 4). Mean declinations with 95% confidence are plotted against magnetostratigraphically determined age at the Xiejia section and compared to the expected declination (dotted line with 95% confidence in gray shaded area) from the poles of Eurasia (Besse and Courtillot, 2002). Most of the clockwise rotation occurred within the indicated horizontal shaded time interval.

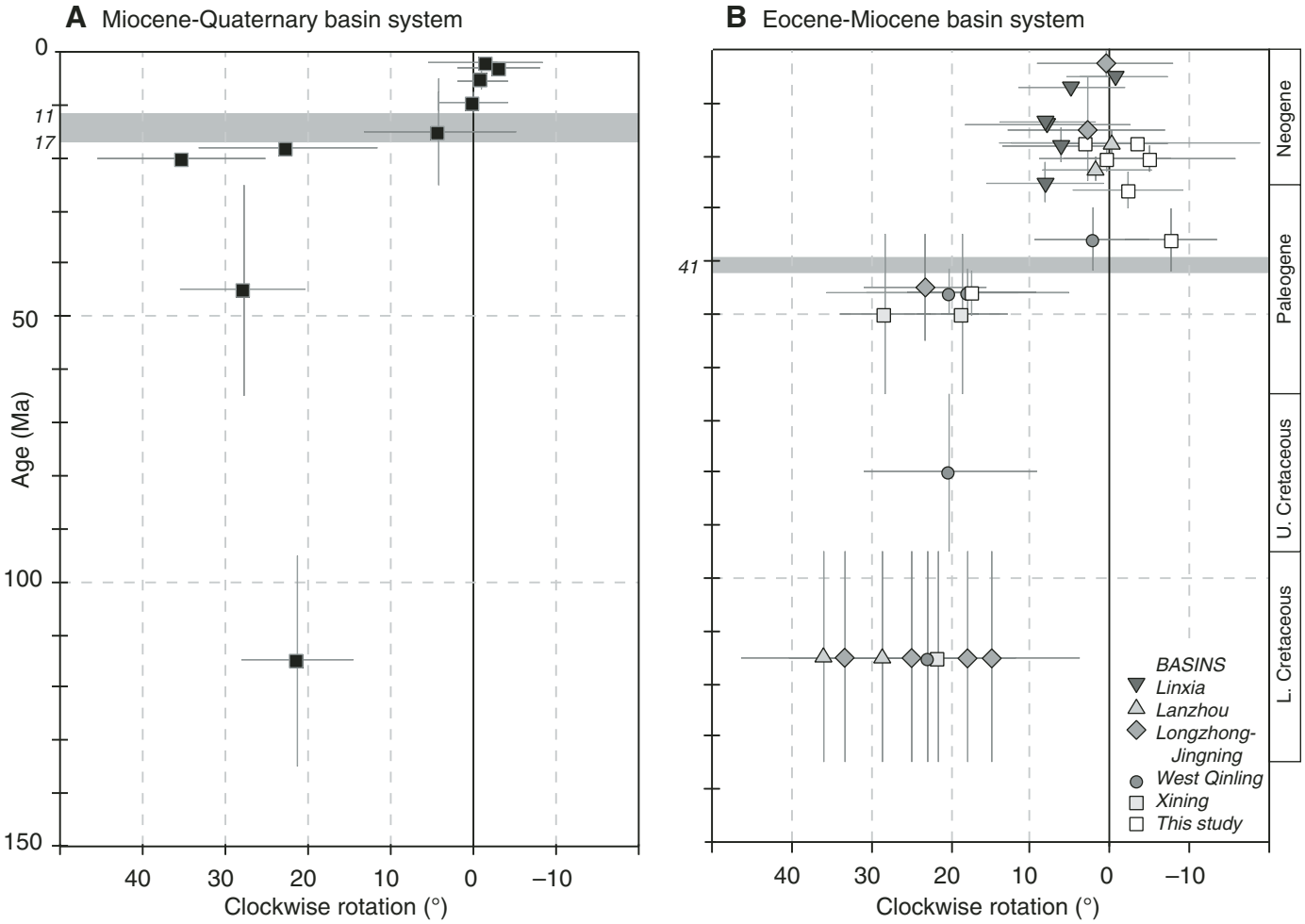

Figure 9. Clockwise rotation relative to the apparent polar wander path of Eurasia as a function of age of the sampled rocks within the northeastern Tibetan Plateau separated in (A) the Paleocene-Miocene basin system and (B) the Miocene-Quaternary basin system (data from Table 1). Thin black lines indicate 95% error bars in clockwise rotation and uncertainty in age (or age span for magnetostratigraphic results; see Table 1). Shaded horizontal areas indicate age range of tectonic rotation.

Regional Tectonic Context of the Early Eocene and Mid-Miocene Rotation Events

The timing brackets on the deformation events outlined by the two distinct rotation phases (at ca. 41 Ma and 17–11 Ma) support previous tectonic interpretations proposed for this region. The younger event that affected the Miocene-Quaternary basin system west of the Laji Shan range can be associated with documented onset of sediment accumulation in the Miocene to Quaternary compressional to transpressional setting (Fang et al., 2005; Yan et al., 2006). This deformation was coeval with widespread middle to late Miocene transpressional activity on various faults and associated range uplift in the northeastern Tibetan Plateau (e.g., George et al., 2001; Kirby et al., 2002; Pares et al., 2003). This activity is well documented in the Kunlun fault system, the Altyn Tagh fault system, and the Qilian Shan belt, possibly resulting from northeastward propagation of deformation of the Indian-Asia collision and Tibetan Plateau uplift (Fig. 1; Meyer et al., 1998; Tapponnier et al., 2001). The tectonic mechanism responsible for clockwise rotation of the Miocene-Quaternary basins must have been associated with crustal deformation on the bounding Laji Shan thrusts. We speculate, based on the absence of Miocene or younger rotation both in the Qaidam Basin to the west (Dupont-Nivet et al., 2002a, 2003) and in the Longzhong Basin to the east, that the Gonghe-Guide-Xunhua Basins may have rotated with crustal slivers in a regional N-S–trending right-lateral shear system driven by differential northward convergence at the eastern margin of the Qaidam Basin (Dupont-Nivet et al., 2004; England and Molnar, 1990).

Early Tertiary tectonic events related to the Paleocene-Miocene basin systems are still poorly understood and documented. Eocene deformation and subsidence in the Xining Basin and the central and northern Tibetan Plateau have been attributed to early propagation of deformation from the

India-Asia collision (Horton et al., 2003; Spurlin et al., 2005; Liu et al., 2003; Dai et al., 2006). Alternatively, the Paleogene may have been a major period of tectonic activity in the Qinling Shan, with widespread Eocene sedimentation in half-graben basins such as the Weihe graben in the Ordos block directly adjacent to the east of the Longzhong Basin (Fig. 1; Bellier et al., 1991; Ratschbacher et al., 2003; Zhang et al., 1998). This deformation has been attributed to far-field effects of back-arc rifting associated with Pacific-Eurasia convergence, which reached a minimum between 53.0 and 39.5 Ma (Allen et al., 1997; Northrup et al., 1995). Although both the Indian-Asia collision and the Pacific margin were located over 2000 km from the Qinling Shan region, it has been suggested that the Paleogene stress field in the Qinling Shan region resulted from the combined effects of Pacific subduction and the India-Asia collision (Ratschbacher et al., 2003). This geodynamic setting may have prompted opening of basins and Eocene clockwise rotations through large-scale N-S–trending dextral shear associated with the accommodation of the penetration of India into Asia (Fournier et al., 2004; Schellart and Lister, 2005). Further assessment of structural features associated with the Paleocene-Miocene basin system is necessary to establish the tectonic mechanism driving clockwise rotations.

ACKNOWLEDGMENTS

We thank R. Molina Garza and J. Geissman for detailed and thoughtful reviews. This work was co-supported by a European Union Marie Curie Fellowship and Netherlands Organization for Scientific Research (NWO) grants to G. Dupont-Nivet and S. Dai, and the Knowledge Innovation Program of the Chinese Academy of Sciences (Grant No. kzcx2-yw-104), the funds of the National Science Foundation of China (40571017, 40721061, 40334038), National Key Project for Basic Research (2005CB422000), and Key Project of Science and Technology of the Ministry of Education of China (grant no. 306016). We thank Meng QingQuan, Cheng Yu, and Tang Yuhu for field assistance.

REFERENCES CITED

Allen, M.B., Macdonald, D.I.M., Xun, Z., Vincent, S.J., and Brouet-Menzies, C., 1997, Early Cenozoic two-phase extension and late Cenozoic thermal subsidence and inversion of the Bohai Basin, northern China: Marine and Petroleum Geology, v. 14, p. 951–972, doi: 10.1016/S0264-8172(97)00027-5.

Argand, E., 1924, La tectonique de l'Asie: Compte-rendu du 13ème Congrès Géologique International, Brussel, v. 1, p. 171–372.

Avouac, J.P., and Tapponnier, P., 1993, Kinematic model of active deformation in central Asia: Geophysical Research Letters, v. 20, p. 895–898, doi: 10.1029/93GL00128.

Beck, M.E., 1980, Paleomagnetic record of plate-margin tectonic processes along the western edge of North America: Journal of Geophysical Research, v. 85, p. 7115–7131, doi: 10.1029/JB085iB12p07115.

Bellier, O., Vergely, P., Mercier, J.L., Ning, C.C., Deng, N.G., Yi, M.C., and Long, C.X., 1991, Analyse tectonique et sedimentaire dans les monts Li Shan (province du Shaanxi-Chine du Nord): Datation des regimes tectoniques extensifs dans le graben de la Weihe: Bulletin de la Société Géologique de France, v. 162, p. 101–112.

Besse, J., and Courtillot, V., 2002, Apparent and true polar wander and the geometry of the geomagnetic field in the last 200 million years: Journal of Geophysical Research, v. 107(B11), no. 2300, doi: 10.1029/2000JB000050.

Cogné, J.P., Halim, N., Chen, Y., and Courtillot, V., 1999, Resolving the problem of shallow magnetizations of Tertiary age in Asia: Insights from paleomagnetic data from the Qiangtang, Kunlun, and Qaidam blocks (Tibet, China), and a new hypothesis: Journal of Geophysical Research, v. 104, p. 17,715–17,734, doi: 10.1029/1999JB900153.

Dai, S., Fang, X., Dupont-Nivet, G., Song, C., Gao, J., Krijgsman, W., Langereis, C., and Zhang, W., 2006, Magnetostratigraphy of Cenozoic sediments from the Xining Basin: Tectonic implications for the northeastern Tibetan Plateau: Journal of Geophysical Research, v. 111, doi: 10.1029/2005JB004187.

Demarest, H.H., 1983, Error analysis of the determination of tectonic rotations from paleomagnetic data: Journal of Geophysical Research, v. 88, p. 4321–4328, doi: 10.1029/JB088iB05p04321.

Dupont-Nivet, G., Guo, Z., Butler, R.F., and Jia, C., 2002a, Discordant paleomagnetic direction in Miocene rocks from the central Tarim Basin: Evidence for local deformation and inclination shallowing: Earth and Planetary Science Letters, v. 199, p. 473–482, doi: 10.1016/S0012-821X(02)00566-6.

Dupont-Nivet, G., Butler, R.F., Yin, A., and Chen, X., 2002b, Paleomagnetism indicates no Neogene rotation of the Qaidam Basin in North Tibet during Indo-Asian Collision: Geology, v. 30, p. 263–266, doi: 10.1130/0091-7613(2002)030<0263:PINNRO>2.0.CO;2.

Dupont-Nivet, G., Butler, R.F., Yin, A., and Chen, X., 2003, Paleomagnetism indicates no Neogene rotation of the northeastern Tibetan Plateau: Journal of Geophysical Research, v. 108, doi: 10.1029/2003JB002399.

Dupont-Nivet, G., Horton, B.K., Zhou, J., Waanders, G.L., Butler, R.F., and Wang, J., 2004, Paleogene clockwise tectonic rotation of the Xining-Lanzhou region, northeastern Tibetan Plateau: Journal of Geophysical Research, v. 109, no. B04401, doi: 10.1029/2003JB002620.

Dupont-Nivet, G., Krijgsman, W., Langereis, C.G., Abels, H.A., Dai, S., and Fang, X., 2007, Tibetan plateau aridification linked to global cooling at the Eocene-Oligocene transition: Nature, v. 445, p. 635–638.

England, P., and Molnar, P., 1990, Right-lateral shear and rotation as the explanation for strike-slip faulting in eastern Tibet: Nature, v. 344, p. 140–142, doi: 10.1038/344140a0.

Fang, X., Garzione, C., Van der Voo, R., Li, J., and Fan, M., 2003, Flexural subsidence by 29 Ma on the NE edge of Tibet from the magnetostratigraphy of Linxia Basin, China: Earth and Planetary Science Letters, v. 210, p. 545–560.

Fang, X., Yan, M., Van der Voo, R., Rea, D.K., Song, C., Pares, J.M., Gao, J., Nie, J., and Dai, S., 2005, Late Cenozoic deformation and uplift of the NE Tibetan Plateau: Evidence from high-resolution magnetostratigraphy of the Guide Basin, Qinghai Province, China: Geological Society of America Bulletin, v. 117, p. 1208–1225, doi: 101130/B25727.1.

Fisher, R.A., 1953, Dispersion on a sphere: Proceedings of the Royal Society of London, Series A, Mathematical and Physical Sciences, v. 217, p. 295–305, doi: 10.1098/rspa.1953.0064.

Flynn, L.J., Downs, W., Opdyke, N.D., Huang, K., Lindsay, E., Ye, J., Xie, G., and Wang, X., 1999, Recent advances in the small mammal biostratigraphy and magnetostratigraphy of Lanzhou Basin: Chinese Science Bulletin, v. 44, supplement, p. 109–117.

Fournier, M., Jolivet, L., Davy, P., and Thomas, J.-C., 2004, Backarc extension and collision: An experimental approach to the tectonics of Asia: Geophysical Journal International, v. 157, p. 871–889.

George, A.D., Marshallsea, S.J., Wyrwoll, K.-H., Chen, J., and Lu, Y., 2001, Miocene cooling in the northern Qilian Shan, northeastern margin of the Tibetan Plateau, revealed by apatite fission-track and vitrinite-reflectance analysis: Geology, v. 29, p. 939–942, doi: 10.1130/0091-7613(2001)029<0939:MCITNQ>2.0.CO;2.

Gilder, S., Chen, Y., and Sen, S., 2001, Oligo-Miocene magnetostratigraphy and rock magnetism of the Xishuigou section, Subei (Gansu Province, western China) and implications for shallow inclinations in central Asia: Journal of Geophysical Research, v. 106, p. 30,505–30,522, doi: 10.1029/2001JB000325.

Halim, N., Cogné, J.P., Chen, Y., Atasiesi, R., Besse, J., Courtillot, V., Gilder, S., Marcoux, J., and Zhao, R.L., 1998, New Cretaceous and early Tertiary paleomagnetic results from Xining-Lanzhou Basin, Kunlun and Qiangtang blocks, China: Implications on the geodynamic evolution of Asia: Journal of Geophysical Research, v. 103, p. 21,025–21,045, doi: 10.1029/98JB01118.

Holt, W.E., Chamot-Rooke, N., Le Pichon, X., Haines, A.J., Shen-Tu, B., and Ren, J., 2000, Velocity field in Asia inferred from Quaternary fault slip rates and global positioning system observations: Journal of Geophysical Research, v. 105, p. 19,185–19,209, doi: 10.1029/2000JB900045.

Horton, B.K., Yin, A., Spurlin, M.S., Zhou, J., and Wang, J., 2003, Paleocene-Eocene syncontractional sedimentation in narrow, lacustrine-dominated basins of east-central Tibet: Geological Society of America Bulletin, v. 114, p. 771–786, doi: 10.1130/0016-7606(2002)114<0771:PESSIN>2.0.CO;2.

Horton, B.K., Dupont-Nivet, G., Zhou, J., Waanders, G.L., Butler, R.F., and Wang, J., 2004, Mesozoic-Cenozoic evolution of the Xining-Minhe and Dangchang Basins, northeastern Tibetan plateau: Magnetostratigraphic and biostratigraphic results: Journal of Geophysical Research, v. 109, no., B04402, doi: 10.1029/2003JB002913.

Kirby, E., Reiners, P.W., Krol, M.A., Whipple, K.X., Hodges, K.V., Farley, K.A., Tang, W., and Chen, Z., 2002, Late Cenozoic evolution of the eastern margin of the Tibetan Plateau: Inferences from Ar/Ar and (U-Th)/He thermochronology: Tectonics, v. 21, doi: 10.1029/2000TC001246.

Kirschvink, J.L., 1980, The least-square line and plane and the analysis of paleomagnetic data: Geophysical Journal of the Royal Astronomical Society, v. 62, p. 699–718.

Liu, Z., Zhao, X., Wang, C., Liu, S., and Yi, H., 2003, Magnetostratigraphy of Tertiary sediments from the Hoh Xil Basin: Implications for the Cenozoic history of the Tibetan Plateau: Geophysical Journal International, v. 154, p. 233–252, doi: 10.1046/j.1365-246X.2003.01986.x.

McFadden, P.L., 1990, A new fold test for palaeomagnetic studies: Geophysical Journal International, v. 103, p. 163–169, doi: 10.1111/j.1365-246X.1990.tb01761.x.

McFadden, P.L., and McElhinny, M.W., 1990, Classification of the reversal test in palaeomagnetism: Geophysical Journal International, v. 103, p. 725–729, doi: 10.1111/j.1365-246X.1990.tb05683.x.

Meyer, B., Tapponnier, P., Bourjot, L., Metivier, F., Gaudemer, Y., Peltzer, G., Shummin, G., and Zhitai, C., 1998, Crustal thickening in the Gansu-Qinghai, lithospheric mantle, oblique and strike-slip controlled growth of the Tibetan Plateau: Geophysical Journal International, v. 135, p. 1–47, doi: 10.1046/j.1365-246X.1998.00567.x.

Molnar, P., England, P., and Martinod, J., 1993, Mantle dynamics, uplift of the Tibetan Plateau, and the Indian monsoon: Reviews of Geophysics, v. 31, p. 357–396, doi: 10.1029/93RG02030.

Northrup, C.J., Royden, L.H., and Burchfiel, B.C., 1995, Motion of the Pacific plate relative to Eurasia and its potential relation to Cenozoic extension along the eastern margin of Eurasia: Geology, v. 23, p. 719–722, doi: 10.1130/0091-7613(1995)023<0719:MOTPPR>2.3.CO;2.

Pares, J.M., Van der Voo, R., Downs, W.R., Yan, M., and Fang, X., 2003, Northeastward growth and uplift of the Tibetan Plateau: Magnetostratigraphic insights from the Guide Basin: Journal of Geophysical Research, v. 108, no. 2017, doi: 10.1029/2001JB001349.

Qinghai Bureau of Geology and Mineral Resources, 1991, Regional geology of the Qinghai Province: Beijing, Geological Publishing House, 662 p.

Qiu, Z., Wang, B., Qiu, Z., Heller, F., Yue, L., Xie, G., and Wang, X., 2001, Land-mammal geochronology and magnetostratigraphy of mid-Tertiary deposits in the Lanzhou Basin, Gansu Province, China: Eclogae Geologicae Helvetiae, v. 94, p. 373–385.

Ratschbacher, L., Hacker, B.R., Calvert, A., Webb, L.E., Grimmera, J.C., McWilliams, M.O., Ireland, T., Dongg, S., and Hug, J., 2003, Tectonics of the Qinling (Central China): Tectonostratigraphy, geochronology, and deformation history: Tectonophysics, v. 366, p. 1–53, doi: 10.1016/S0040-1951(03)00053-2.

Ruddiman, W.F., Kutzbach, J.E., and Prentice, I.C., 1997, Testing climatic effects of orography and CO2 with general circulation and biome models, *in* Ruddiman, W.F., ed., Tectonic uplift and climate change: New York, Plenum Press, p. 203–235.

Schellart, W.P., and Lister, G.S., 2005, The role of the East Asian active margin in widespread extensional and strike-slip deformation in East Asia: Journal of the Geological Society, v. 162, p. 959–972, doi: 10.1144/0016-764904-112.

Spurlin, M.S., Yin, A., Horton, B.K., Zhou, J., and Wang, J., 2005, Structural evolution of the Yushu-Nangqian region and its relationship to syncollisional igneous activity, east-central Tibet: Geological Society of America Bulletin, v. 117, p. 1293–1317, doi: 10.1130/B25572.1.

Tapponnier, P., 2001, Oblique stepwise rise and growth of the Tibetan Plateau: Science, v. 394, p. 1671–1677, doi: 10.1126/science.105978.

Tapponnier, P., Xu, Z., Roger, F., Meyer, B., Arnaud, N., Wittlinger, G., and Yang, J., 2001, Oblique stepwise rise and growth of the Tibetan Plateau: Science, v. 294, p. 1671–1677.

Tauxe, L., 1998, Paleomagnetic Principles and Practice: Dordrecht, Kluwer Academic Publisher, 299 p.

Vandamme, D., 1994, A new method to determine paleosecular variation: Physics of the Earth and Planetary Interiors, v. 85, p. 131–142.

Wang, C., Zhao, X., Liu, Z., Lippert, P.C., Graham, S.A., Coe, R.S., Yi, H., Zhu, L., Liu, S., and Li, Y., 2008, Constraints on the early uplift history of the Tibetan Plateau: Proceedings of the National Academy of Sciences, v. 105, p. 4987–4992.

Yan, M., Van der Voo, R., Fang, X.-M., Pares, J.M., and Rea, D.K., 2006, Paleomagnetic evidence for a mid-Miocene clockwise rotation of about 25° of the Guide Basin area in NE Tibet: Earth and Planetary Science Letters, v. 241, p. 234–247, doi: 10.1016/j.epsl.2005.10.013.

Yang, T., Yang, Z., Sun, Z., and Lin, A., 2002, New Early Cretaceous paleomagnetic results from Qilian orogenic belt and its tectonic implications: Science in China, ser. D, v. 45, p. 565–576.

Yin, A., and Harrison, M.T., 2000, Geologic evolution of the Himalayan-Tibetan orogen: Annual Review of Earth and Planetary Sciences, v. 28, p. 211–280, doi: 10.1146/annurev.earth.28.1.211.

Zhai, Y., and Cai, T., 1984, The Tertiary System of Gansu Province, *in* Wang, Y.M., ed., Gansu Geology: People's Press of Gansu, p. 1–40, http://www.nau.edu/~qsp/will_downs/86.pdf.

Zhang, Y.Q., Mercier, J.L., and Vergely, P., 1998, Extension in the graben systems around the Ordos (China), and its contribution to the extrusion tectonics of South China with respect to Gobi-Mongolia: Tectonophysics, v. 285, p. 41–75, doi: 10.1016/S0040-1951(97)00170-4.

Manuscript Accepted by the Society 04 April 2008